

Fig. 4. Height variations in the region of Iapygia obtained from 3.8-cm radar observations in June ( $-18^\circ$  latitude), July ( $-16^\circ$ ), and late August ( $-14^\circ$ ) 1971. Error bars have been omitted for clarity but may be estimated from the internal consistency of the data. In June, 10- $\mu$ sec baud lengths were used; from July on the data were obtained with 6- $\mu$ sec bauds.

No other data for this region are yet available. A few craters, but no related feature, may be seen in the far-encounter Mariner photographs of this region.

Referring now to Fig. 1c, we see a small but nearly 2-km-deep feature (G) at  $167^\circ$  that correlates well with the northern limit of Titanus Sinus at the boundary between Mare Sirenum and Memnonia. At  $149^\circ$  (feature H) a crater can be seen that corresponds to a very weakly defined shading in the far-encounter photographs. The dominant features of Fig. 1c, however, are the twin "peaks" in Phoenicis Lacus at  $122^\circ$  and  $100^\circ$ . These features are unusually well defined, and the latter in particular offers a surface of extremely high radar reflectivity. The strongest echo strength obtained in the entire data span was observed at  $108^\circ$ . As mentioned earlier, these features appear to be a continuation into the southern hemisphere of the major topographic ridge seen at earlier oppositions in the northern hemisphere.

Repeated attempts to observe echoes in the longitude region  $125^\circ$  to  $121^\circ$  have been unsuccessful. The possibility that echoes from a region of this average slope ( $1^\circ$ ) might be displaced sufficiently in frequency as to lie outside the basic processing bandwidth has been ruled out by looking for

echoes in frequency windows adjacent to the central one. Apparently the surface in this region is either exceedingly rough at the scale of the wavelength used or of extremely low intrinsic reflectivity (or it has a combination of these properties). The short gap evident at  $98^\circ$  was caused by a system failure and has been filled by (unremarkable) observations since the preparation of Fig. 1c. The downslope of the second peak extends from  $95^\circ$  to  $80^\circ$  longitude; it is strongly reflective and falls off smoothly. It is an area apparently free of even small craters. No optical features of prominence can be discerned over the longitude region from  $140^\circ$  to  $80^\circ$  at this latitude.

A surprising result of these observations is the failure to observe any correlation between regions of high radar reflectivity and optically dark areas. Such a correlation has been observed at northern latitudes (1, 2, 8), but it is expected that with the inclusion of these new data the composite correlation may disappear (an exact calculation has not yet been performed).

G. H. PETTENGILL

Department of Earth and Planetary Sciences, Massachusetts Institute of Technology, Cambridge 02139

A. E. E. ROGERS

Haystack Observatory, Northeast Radio Observatory Corporation, Westford, Massachusetts 01886

I. I. SHAPIRO

Department of Earth and Planetary Sciences, Massachusetts Institute of Technology

## Mars Radar Observations, a Preliminary Report

*Abstract. Radar observations of a narrow belt of the surface of Mars, centered at  $16^\circ$  south latitude, show a very rugged terrain, with elevation differences greater than 13 kilometers from peak to valley. For nearby points, the relative altitude is measured to 40 meters at best; the precision is worse for points at different latitudes, or widely separated in longitude, because of orbital uncertainties. Some of the larger craters have been resolved, and their depth and, in some cases, the height of the raised rim have been measured. Where high resolution photographs are available, the correlation is excellent.*

Mars, during its opposition this summer, passed closer to the earth than it will again for 17 years. We have taken advantage of this favorable approach to conduct an extensive set of radar measurements at the Jet Propulsion Laboratory's Goldstone Tracking Station.

Mars has been studied by radar at each opposition since 1963 (1, 2). The

## References and Notes

1. G. H. Pettengill, C. C. Counselman, I. P. Rainville, I. I. Shapiro, *Astron. J.* **74**, 461 (1969).
2. A. E. E. Rogers, M. E. Ash, C. C. Counselman, I. I. Shapiro, G. H. Pettengill, *Radio Sci.* **5**, 465 (1970).
3. R. M. Goldstein, W. G. Melbourne, G. A. Morris, G. S. Downs, D. A. O'Handley, *ibid.*, p. 475.
4. Negative values of latitude correspond to south Martian latitude; all longitudes are given as increasing to the west. (These are the standard International Astronomical Union conventions.)
5. Observations made subsequently suggest that the topography at longitudes slightly west of (that is, greater than)  $60^\circ$  is shown as 0.3 km too low, whereas the topography at longitudes slightly east of (less than)  $60^\circ$  is shown as 0.3 km too high, as compared to the average. The intervening topography would be proportionately less affected.
6. The general behavior of the surface height variations in the region extending eastward from  $40^\circ$  to  $350^\circ$  longitude is consistent with earlier deductions made from the Mariner ultraviolet spectrometer measurements [C. A. Barth and C. W. Hord, *Science* **173**, 197 (1971)].
7. The altitude transition as this edge passes through the subearth point occurs in less than 20 seconds of time, which offers the attractive possibility of extremely accurate cartographic calibration.
8. R. B. Dyce, G. H. Pettengill, A. D. Sanchez, *Astron. J.* **72**, 771 (1967); R. M. Goldstein and W. F. Gillmore, *Science* **141**, 1171 (1963); see also C. Sagan, J. B. Pollack, R. M. Goldstein, *Astron. J.* **72**, 20 (1967).
9. Figure 3 is reproduced by permission of Mr. C. A. Cross of the Rand Corporation (Rand Publ. R-757-NASA).
10. We thank the staff of the Haystack Observatory for their valuable contribution to an often tedious observing program. Particular appreciation is owed to the observers H. H. Danforth, J. J. Kollasch, and B. G. Leslie, as well as to R. A. Brockelman for development of the computer program used in observation. The improved instrumentation that made possible a delay resolution of 6  $\mu$ sec was developed by J. Levine and R. P. Ingalls. The Haystack Observatory is operated under agreement with the Massachusetts Institute of Technology by the Northeast Radio Observatory Corporation with support from NSF grant GP-25865 and NASA grant NGR-22-174-003.

21 September 1971; revised 4 November 1971 ■

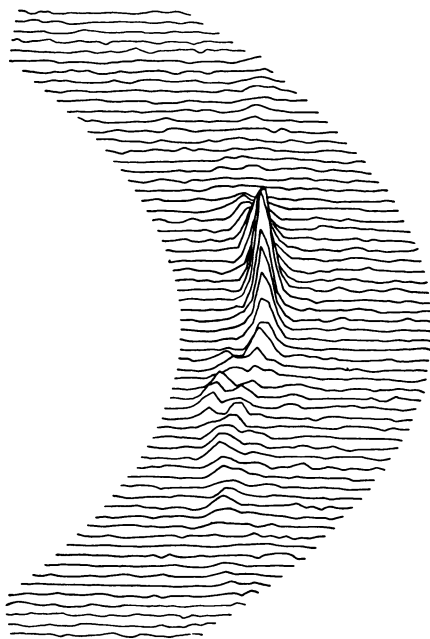


Fig. 1. Radar echo power partitioned into range and Doppler cells. Each line represents a vertical slice (9.4 km wide) through Mars. The earth is far to the left, the center of Mars to the right. Range points are separated by 450 m. A level surface would appear as pulses aligned vertically on the plot.

time of flight. Then the antenna is switched to a receiver for an equal period of time, to collect the reflected signals. The send and receive cycles alternate throughout the observing night.

As Mars rotates, the subradar point (the point on Mars closest to the radar station) traces out an arc of a latitude circle. About  $90^\circ$  of longitude can be examined in one night. Since Mars rotates slightly more slowly than the earth, observations several nights later relate to a displaced arc of the latitude circle. In about 40 nights, the original longitude returns to view, but by then the latitude circle has changed. During the current set of experiments, the subradar latitude began at  $-17^\circ$ , advanced to  $-14^\circ$ , and will return to  $-20^\circ$ . By International Astronomical Union convention, south martian latitudes are indicated by negative latitude values. Observations were scheduled for every third or fourth night from early June through mid-October.

Special-purpose computing machinery is used to partition the received echo power into a two-dimensional array of cells. Range, or time delay, is the first dimension. Range contours on the surface consist of a set of circles concentric to the subradar point. The contours are spaced 450 m apart in range, and the signal processing system has a response at half power of about the same width. Doppler frequency shift, caused by Mars' rotation, forms the second dimension. Seen edgewise by the radar, the Doppler contours are also concentric circles, which are parallel to the effective axis of rotation. These circles thus divide the echo power along strips running almost due north and south. Our resolution in this dimension is 9.4 km. Every 30 seconds of each receiving cycle, an array of 32 range by 64 Doppler cells is recorded. Surface elements, carried by Mars' rotation, move through less than one Doppler strip in this 30-second interval, so that blurring of the recording is minimized.

Figure 1 is a sample of one such data array. It corresponds to a disk about  $10^\circ$  in diameter on Mars. Range is plotted along the abscissa and echo power along the ordinate. Each line corresponds to one Doppler strip and the lines have been displaced in such a manner that latitude circles of Mars

of interest as the Mariner 9 spacecraft approaches encounter with Mars.

The radar parameters are: transmitted power, 300 kw; two-way antenna gain, 124 db; system noise temperature,  $23^\circ\text{K}$ ; wavelength, 12.5 cm. These parameters represent a gain of a factor of 160 since 1963. Our experimental procedure consists of a series of send and receive cycles. Radio waves of 12.5 cm are beamed toward Mars for 6.5 to 11 minutes, the round-trip

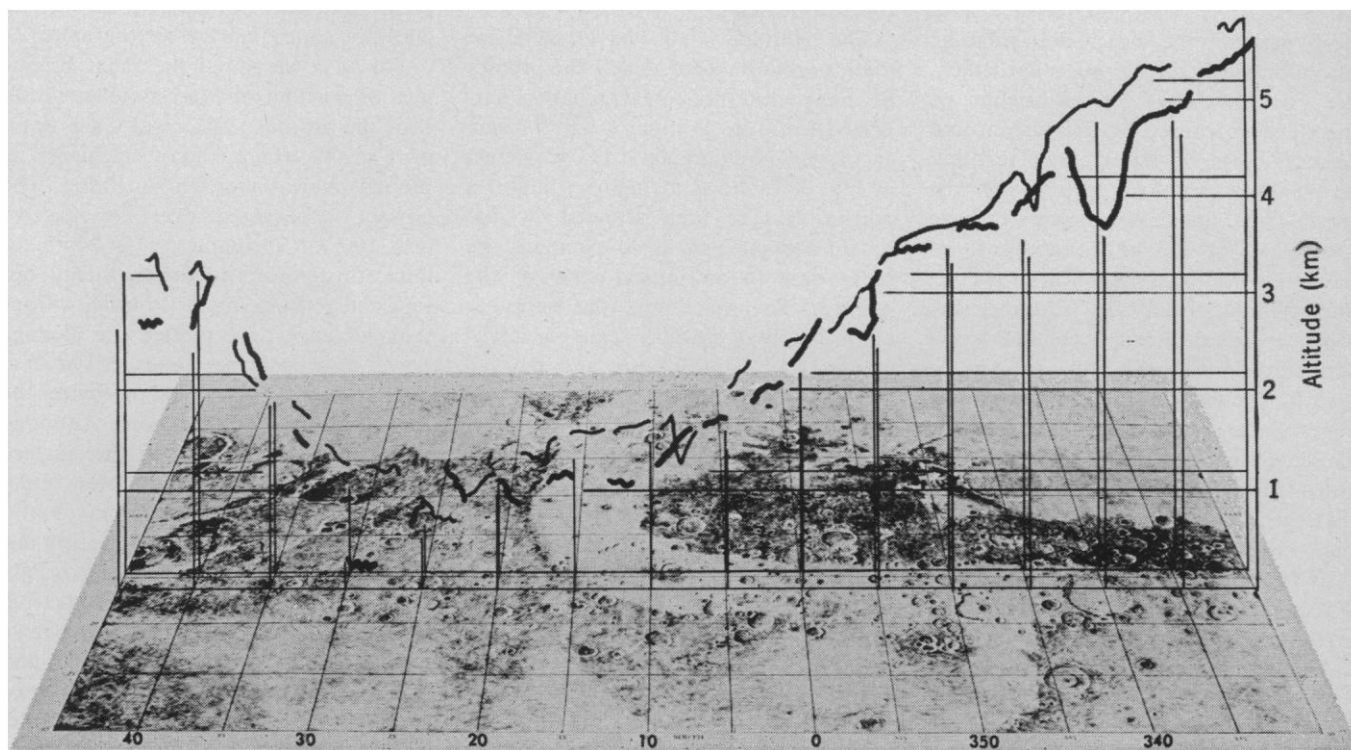


Fig. 2. Two altitude profiles drawn over a Mars chart interpreted from Mariner 6 and 7 photographs.

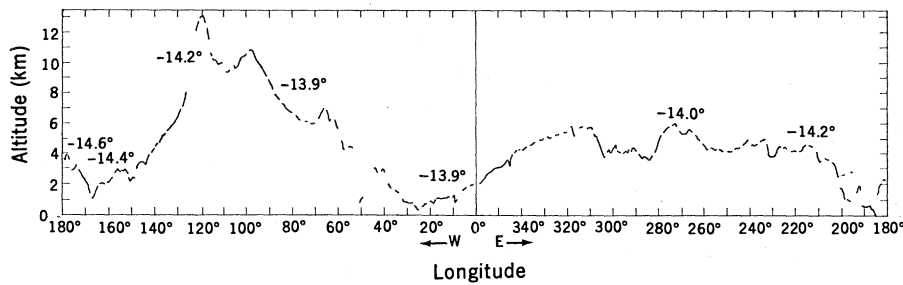


Fig. 3. Profile of altitude as a function of longitude for Mars. The International Astronomical Union coordinate system is used.

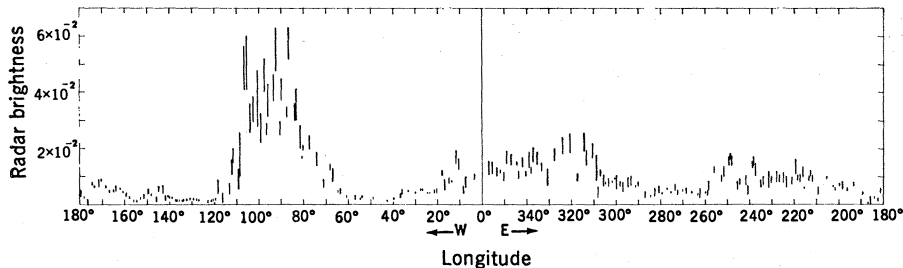


Fig. 4. A radar brightness profile over the region shown in Fig. 3.

would correspond to straight vertical lines in the plot. In this representation, altitude variations along the subradar track can be seen directly on the plot as variations from a vertical line.

Figure 1 does not show typical data. The altitude profile is unusually irregular. Furthermore, the strongest echo is not from the front cap but from points well back from it. We attribute these characteristics to a large martian crater, situated such that the subradar track crosses it between its center and its edge. The strongest echo comes from parts of the crater floor that lie on both sides of the subradar track. We can show that the bifurcation of the ridges is caused by the eastern and western parts of the crater floor that lie wholly north (or south) of the track. Thus, this crater appears to have a diameter of 250 km, although it intercepts a width of only 130 km along the subradar track. In addition, the crater is about 2 km deep and has a rim elevation of 0.9 km, as can be seen by the displacement of the leading edges. Since strong echoes are generally caused by smooth surface elements oriented toward the radar, we conclude that the crater floor is much smoother than the top. This crater is located at 185°W longitude and either  $-13^\circ$  or  $-16^\circ$  latitude. Smaller topographic details can also be seen in Fig. 1.

The altitude estimates, which we report below, were formed from a small set of data points near the front cap, where the sensitivity is greatest. This gives an effective resolution on the

martian surface of a disk of about 100-km diameter. Our altitude resolution is much finer. It is determined by both the spacing of the range contours and the signal-to-noise ratio of the echoes. At times when the subradar latitude was not changing too rapidly and the echo strength was high, a repeatability from one observing night to another of 40 m was obtained. When the latitude was changing more rapidly, the repeatability was poorer, a fact which we attribute to the viewing of somewhat different surface elements.

The altitude data have sufficient resolution to indicate clearly the profiles of many craters. A Mars chart, interpreted from the Mariner 6 and 7 near-encounter photographs (3), is shown in Fig. 2. It shows at high resolution a portion of the area scanned by the radar, and enables us to compare the radar data to an optical view of the surface. The tracks of the subradar point for two altitude scans ( $-13.8^\circ$  and  $-16.1^\circ$  latitude) are also marked in Fig. 2, and plotted above the tracks are our altitude estimates for that part of Mars. The ordinate is in kilometers above an arbitrary radius. An estimate of the actual radius at this latitude awaits a least-squares fit of the orbit and figure of Mars to the entire collection of data. Gaps in the data are the result of the alternation of send and receive cycles and of spacings of more than four nights between some observations.

The most striking feature of these plots is the large crater at 340°W. It

is crossed by the lower scan, which resolves it easily. The crater lies on an east-west slope of  $0.09^\circ$ , is 0.9 km deep, and has a raised rim on the downhill side. The upper scan just misses this crater, but shows an indication of its rim. At 344°W, the upper scan shows an anomaly, at the limit of resolution, that corresponds to overlapping craters on the Mars chart. A smaller crater, at 8°W, is also indicated by the upper scan. In general, there is a very close correlation between the radar data and the chart. An exception is the deep hole indicated by the lower scan at 29°W. No anomaly appears at that location on the chart.

Since the correlation between radar and optical data is high where optical data are available, we expect it to remain high elsewhere. Figure 3 is a plot of altitudes for 360° of longitude and  $-13.8^\circ$  to  $-14.6^\circ$  of latitude. It repeats the overall rugged profiles measured earlier at northern latitudes (2). More than 13 km separates the highest altitude from the lowest in this series of measurements. The highest peak occurs at 120°W, only 35° east of one of the lowest areas. Between these extreme locations lies a gradually increasing slope averaging  $0.26^\circ$  and reaching a maximum of  $1.3^\circ$ . We attribute much of the fine structure in this plot to craters. Indeed, the larger ones at 230°W and 188°W are identifiable on the Mariner far-encounter pictures. The very large craterlike object that extends 1800 km and is centered at 293°W does not appear on the photographs.

We have measured the radar brightness of portions of Mars simultaneously with the altitude. The results are given in Fig. 4, where radar brightness is plotted against martian longitude. The power is measured over an effective disk 100 km in diameter. As Mars rotates, this power fluctuates widely but repeatedly from night to night. Consequently, we have plotted the average power over each receive cycle. The bars on the figure correspond to twice the root-mean-square fluctuations. Although the dielectric constant of the surface affects the echoes, they must be dominated by the degree of surface smoothness. Since only the region very near the subradar point is examined, any roughness would scatter energy away from the earth. Thus, rocky, boulder-strewn areas would be dark to the radar. Smooth crater floors would be expected to be bright to radar, but the crater walls would not.

Because radar brightness is deter-

mined by small-scale structure, we expect little relationship of this profile to the measurements made at northern latitudes. Little was found, except for the area between 120° and 140°W, which was dark to radar at both latitudes.

G. S. DOWNS  
R. M. GOLDSTEIN  
R. R. GREEN  
G. A. MORRIS

*Jet Propulsion Laboratory,  
California Institute of Technology,  
Pasadena 91103*

## Cave Development during a Catastrophic Storm in the Great Valley of Virginia

*Abstract. Observations made before and after a catastrophic storm support the conclusion that caves receiving storm recharge may be significantly developed in the vadose zone by the processes of mass transfer. These processes are greatly accelerated during times of major floods. Evidence indicates that in ancient times floods of similar magnitude have occurred.*

We present here observations which indicate that storm runoff is an important factor in the development of caves in the vadose zone. The effects of a single high-magnitude storm and evidence of similar events in the past are reported.

On 17 August 1969, Hurricane Camille, a relatively small but extremely intense storm, blew into the United States along the coast of Mississippi. The damage it produced, its extremely low barometric pressure (901 mb), and its high surface wind velocities [172+ miles per hour (275+ km per hour)] may have gained it the title of "this century's greatest hurricane" (1). On the evening of 18 August Camille left northeastern Mississippi as a tropical depression (winds less than 38 miles per hour) and arched northeastward through Tennessee and Kentucky; it grazed the southern edge of West Virginia and moved into Virginia.

Camille's cyclonic circulation fed the storm into the northeast-trending Great Valley system where it encountered a relatively warm mass of moist maritime air, the orographic effect produced by the Blue Ridge Mountains, and the influence of a cold front approaching from the north (2). At several locations in Virginia 25 to 28 inches (63.5 to 71 cm) of rainfall in 8 hours were recorded, and in one instance 31 inches in a similar time interval was reported. The maximum rainfall has a return period "well in excess of 1000 years"

### References and Notes

1. R. M. Goldstein and W. F. Gillmore, *Science* **141**, 1171 (1963); R. M. Goldstein, *ibid.* **150**, 1715 (1965).
  2. G. H. Pettengill, C. C. Counselman, L. P. Rainville, I. I. Shapiro, *Astron. J.* **74**, 461 (1969); R. M. Goldstein, W. G. Melbourne, G. A. Morris, G. S. Downs, D. A. O'Handley, *Radio Sci.* **5**, 475 (1970); A. E. E. Rogers, M. E. Ash, C. C. Counselman, I. I. Shapiro, G. H. Pettengill, *ibid.*, p. 465.
  3. The original of the Mars chart was prepared by C. A. Cross and M. E. Davies of the Rand Corporation, under contract to the National Aeronautics and Space Administration.
  4. This report presents the results of one phase of research carried out at the Jet Propulsion Laboratory under NASA contract NAS 7-100.
- 12 October 1971 ■

the hydrology of a stream located in Cave Springs Cave, about 1 mile northwest of Lexington, Virginia, in a karst terrain underlain by the New Market and Lincolnshire formations. The stream flows through approximately 2000 feet (610 m) of the cave's passageways and occupies entrenched meanders along some reaches. It enters and leaves the cave through joints enlarged by solution, eventually reappearing at the surface a short distance away whereupon it flows into the Maury River.

Before the storm, the stream had a maximum depth of 2 to 3 feet, had an average depth of less than a foot, and carried a load consisting predominantly of mud containing some well-rounded chert pebbles. The stream load consisted of the typical insoluble residue to be expected from the limestone bedrock. Apparently the feeding joint system would not permit coarser alluvium access to the cave. Like many of the caves in the region, Cave Springs Cave is decorated with those kinds of speleothemic features that commonly adorn limestone caverns. These features testify to the supersaturation of waters with respect to calcium carbonate during at least part of the cave's history. The walls of the cave along the stream exhibited smooth, subdued, polygonal scallops (5). These features, which in the past have been interpreted as evidence of mechanical erosion (6), have in recent years been attributed to mass transfer on a molecular scale, that is, solution (5, 7). Most of the scallops were masked by a patina of mud ranging in color

(3); the peak discharge of many streams in the storm area has a comparable return period. New high-water marks were established for many of the streams in the James, Potomac, Rappahannock, and York river basins (4).

Cataclysmic changes were not confined to the surface, for much of the Great Valley contains karst topography with substantial subterranean drainage. Figure 1 shows a collapse feature which formed during the Camille storm near Lexington, Virginia.

Prior to the storm, we were studying



Fig. 1. Dolina or sinkhole which formed near Lexington, Virginia, during the Camille storm. [Courtesy of E. W. Spencer, Department of Geology, Washington and Lee University, Lexington, Virginia]